

Optimization of autogenous shrinkage and microstructure for Ultra-High Performance Concrete (UHPC) based on appropriate application of porous pumice

Kaizhi Liu ^{a,b}, Rui Yu ^{a,c,*}, Zhonghe Shui ^{a,c}, Xiaosheng Li ^{a,b}, Cheng Guo ^{a,b}, Bailian Yu ^{a,b}, Shuo Wu ^a

^a State Key Laboratory of Silicate Materials for Architectures, Wuhan University of Technology, Wuhan 430070, China

^b School of Materials Science and Engineering, Wuhan University of Technology, Wuhan 430070, China

^c Wuhan University of Technology Advanced Engineering Technology Research Institute of Zhongshan City, Xiangxing Road 6, 528400 Zhongshan, Guangdong, China

HIGHLIGHTS

- Pore parameters characterization of pumice porous material is executed.
- An optimum design of pumice-based UHPC system is presented.
- The internal curing effect generated from pumice material is investigated.
- Multiple evaluation of pore structure for the development of UHPC is done.
- Multiple analytical techniques are applied to characterize the UHPC ITZ.

ARTICLE INFO

Article history:

Received 28 October 2018

Received in revised form 26 March 2019

Accepted 8 April 2019

Keywords:

Ultra-High Performance Concrete (UHPC)

Autogenous shrinkage

Microstructure

Porous pumice stone material

Optimization

ABSTRACT

In this study, optimization of autogenous shrinkage and microstructure for Ultra-High Performance Concrete (UHPC) based on appropriate application of porous pumice is addressed. The pumices with different water absorption rates are utilized to replace river sand by 10%, 20% and 30%, and its effect on the properties of the developed UHPC is investigated. The obtained experimental results show that the inclusion of pre-wetting pumice (particle size distribution is 0.6–1.25 mm) can significantly reduce the autogenous shrinkage of UHPC, without decrease the mechanical properties. Mercury Intrusion Porosimetry and Computed Tomography results indicate that the incorporation of 0.6–1.25 mm hydrous pumice can refine the pore structure and increase the fraction of interconnected pores. Environmental Scanning Electron Microscope, Super-high Magnification Lens Zoom 3D Microscope and Electron BackScattered Diffraction images revealed that the interfacial transition zone (ITZ) skeleton between hydrous pumice and UHPC paste is obviously improved.

© 2019 Elsevier Ltd. All rights reserved.

1. Introduction

Ultra-High Performance Concrete (UHPC) is a new type of cement-based material based on the closest packing between the component particles [1–4]. Compared to ordinary or high-performance concrete, UHPC has many outstanding advantages, such as rapid early strength development, high post-strength and high compactness, which cause that it is an advanced building composite material with good application prospects in the near

future. Nevertheless, the disadvantages of the UHPC in current stage should never be ignored, e.g. shrinkage.

As commonly known, shrinkage is the inevitable and spontaneous volume deformation of concrete in the process of gradual hardening. Due to some typical characteristics for UHPC production (e.g. low water-binder ratio, high cementitious material content, incorporation of superplasticizer and elimination of coarse aggregate), there is a great difference in the hydration process and microstructure development between UHPC and ordinary concrete, which on one hand can improve the mechanical properties and durability of UHPC, and on the other hand could lead to a large early shrinkage [5,6]. UHPC with low water-binder ratio shows self-desiccation in a few hours of molding, leading to a rapid development of autogenous shrinkage at early age [7,8]. Its 7 d

* Corresponding author at: State Key Laboratory of Silicate Materials for Architectures, Wuhan University of Technology, Wuhan 430070, China.

E-mail address: r.yu@whut.edu.cn (R. Yu).

autogenous shrinkage can reach 500–1500 μe , which is an order of magnitude larger than the drying shrinkage. Therefore, for UHPC, the autogenous shrinkage mainly dominates the total contraction [9–11]. The relatively large shrinkage can negatively affect the concrete volume stability and strength development, and further resulting in concrete internal micro-cracks, which can significantly deteriorate the durability of UHPC. Therefore, controlling the volume contraction of UHPC plays a vital role in improving its durability and applicability in the near future.

Recently, the main technical means to reduce the autogenous shrinkage of UHPC can be summarized as follows: 1) inclusion of supplementary cementitious material (SCM); 2) use of expansion agent (EA); 3) application of shrinkage reducing admixture (SRA); 4) fiber toughening; 5) appropriate curing condition; 6) internal curing. To be specific, the introduction of fly ash (FA), silica fume (SF), and ground granulated blast furnace slag (GGBFS) multiple systems can effectively reduce the autogenous shrinkage of UHPC through the filling effect and the pozzolanic effect [12–16]. The reaction of the EA itself or reaction with other components in the cement produces a pre-compressive stress in the hardening process of the concrete, substantially offsets the tensile stress occurring in the concrete, thereby realizing the compensation shrinkage of the concrete [17,18,21]. The SRA can reduce the surface tension of water in concrete pores, thereby reducing the pressure and shrinkage stress of the pores, and effectively inhibiting the autogenous shrinkage and drying shrinkage of UHPC [19–21]. Fiber toughening can also play a role in reducing the autogenous shrinkage of concrete through the restraint of fibers [22,23]. The heating or steaming can obviously promote the UHPC hydration, which causes that its late properties development is slow and the shrinkage is slight [24–27]. However, all the mentioned strategies above have their own drawbacks. Such as: 1) the compatibility between EA and concrete is questionable; 2) the SRA can reduce the early strength of concrete, extend the setting time, sometimes interact with other admixtures; 3) fiber toughening is difficult to radically solve the problem of self-desiccation inside UHPC; 4) the curing regime, including thermal curing and steam curing, will inhibit the subsequent strength development of concrete and adversely affect its durability.

Based on available literature, it can be noticed that internal curing is an effective method to delay the self-desiccation inside concrete, and fundamentally solve the problem of excessive autogenous shrinkage of UHPC. At present, superabsorbent polymer (SAP), rice husk ash (RHA), and various lightweight aggregates (LWAs) are mainly used in UHPC as internal curing materials. SAP can validly compensate the relative humidity inside the concrete, thus remarkably reducing its autogenous shrinkage [15,27–31]. RHA has fine biological mesoporous structure, micro-aggregate effect and pozzolanic activity, which can be used as active admixture to roughly offset the autogenous shrinking of UHPC [32–35]. Nevertheless, SAP is accompanied by obvious volume change during the process of water absorption and release. The introduction of holes after release of water by SAP will reduce the compactness of UHPC, resulting in the loss of strength. The properties of RHA is greatly influenced by the conditions of origin and combustion, and the effect of concrete performance has great fluctuation, which limits its applicability in some degree. Hence, more reliable approach to effectively reduce UHPC autogenous shrinking is urgent needed.

Some investigations have already demonstrated that LWAs after pre-wetting treatment can significantly reduce the autogenous shrinkage of UHPC. For instance, the use of saturated coral aggregate (SCA) as practical replacement of quartz sand has been shown to effectively mitigate the autogenous shrinkage in UHPC, while the mechanical properties were deteriorated by the addition of SCA [36]. Under the saturated water absorption state, the

expanded shale can promote the continuous hydration of the UHPC system after 28 days, and the best effect is achieved when the content is 25%. The 91 d compressive strength of UHPC can reach 168 MPa, while its 28 d autogenous shrinkage is 365 μe [37]. In the cement paste with low water-binder ratio, regarding the time when internal relative humidity (RH) begins to drop as “time-zero”, the cement paste blended by 20% zeolite shows a higher internal RH and a slightly less autogenous shrinkage than the primitive mortar at 3 days after mixing [38]. Pumice stone is a kind of natural porous mineral material with very rich pore structures, and has been used as internal curing agent in ordinary and high strength concrete. Recent studies demonstrate that pre-wetting pumice can significantly reduce the autogenous shrinkage of concrete, but it has an adverse effect on its compressive strength. At the same time, the particle size of the selected pumice has a great influence on the curing efficiency of concrete [39–45]. Nevertheless, there are great differences between UHPC and ordinary or high strength concrete, and whether these experiences are applicable to UHPC is still uncertain. Pumice has great advantages and potential as an internal curing agent in UHPC. However, very limited information regarding the positive effect of pumice on UHPC autogenous shrinkage can be easily found in literature.

Consequently, in this paper, pumice with different water absorption rates, under unsaturated water absorption and saturated water absorption conditions, respectively, are utilized to replace river sand with similar particle size distribution. Then, the properties (e.g. working performance, mechanical properties and autogenous shrinkage) of the developed UHPC are studied. Based on the characterization and analysis of microstructure, hydration process and pore development of hardened paste, the intrinsic mechanisms of the pumice internal curing process in UHPC are investigated.

2. Materials and methods

2.1. Materials

The cementitious materials utilized in this study include OPC 52.5 cement, fly ash (FA) and silica fume (SF). Besides, two types of natural river sand and pumice stone with different particle size range (0–0.6 mm and 0.6–1.25 mm, respectively) are utilized as fine aggregates. The chemical compositions of cement, fly ash, silica fume, river sand and pumice stone are presented in Table 1. A polycarboxylic ether based superplasticizer (SP) is adopted to satisfy the flowability demand of the designed UHPC.

Pumice is a volcanic vitreous effusion rock with rich pores, which has the characteristics of light weight, porous, high water absorption, acid-proof alkaline, anti-corrosive and low thermal conductivity, etc [46–49]. These features can well meet the requirements of internal curing materials. In this study, the pore structure, pore size distribution and porosity of pumice are characterized by Environmental Scanning Electron Microscope (ESEM), Super-high Magnification Lens Zoom 3D Microscope (3D M), Computed Tomography (CT), Mercury Intrusion Porosimetry (MIP) and N_2 -Sorption Isotherm (BET – BJH). Thermal analysis (TG – DTG) is employed to test the water release rate of pumice with different particle sizes, under the heating rate of 0.5 $^{\circ}\text{C}/\text{min}$ and temperature range of 15 $^{\circ}\text{C}$ –80 $^{\circ}\text{C}$.

The ESEM images of the used pumice stone are shown in Fig. 1. As can be noticed that the pumice stone is a natural porous mineral material with rough surface and highly developed pore structure just like cellular texture, among which the macro-pore structure is the chief component. The pore distribution is not uniform and the size varies greatly, mostly open pores. The open holes in the interior may cause that the used pumice has a large water absorption rate. The pore diameter can be changed between $n \times n \times 10^2 \mu\text{m}$, generally spherical or ellipsoidal pores, the inner wall is relatively smooth. The 3D M pictures of the employed pumice are given in Fig. 2. It is clear that the channel structure of the pumice is elongated and oriented to form a flow framework. The space of these cylinder and cylindroid columns can ensure that the pumice channel has a strong capacity of water storage and water retention, and provides a guarantee for periodic water release with the change of the external environment. The obtained CT results are presented in Fig. 3. It could be found that the pumice has a three-dimensional and multi-aperture framework, the porosity is up to 56.0%, the porosity connectivity is 99.8%. The porosity of pumice is so abundant and developed, meanwhile the pore connectivity is such high. Therefore, it can be predicted that when hydrous pumice is included into UHPC, contact area between the water release region and UHPC matrix can be increased, and the internal curing efficiency could be simultaneously enhanced.

Table 1

The chemical compositions of cementitious materials and fine aggregates (wt. %).

Compositions	Na ₂ O	MgO	Al ₂ O ₃	SiO ₂	P ₂ O ₅	SO ₃	K ₂ O	CaO	Fe ₂ O ₃	LOI
Cement	0.09	1.61	4.18	19.20	0.09	3.35	0.78	64.93	3.32	2.49
Silica fume	0.13	0.47	0.25	94.65	0.17	0.69	0.84	0.36	0.15	2.29
Fly ash	0.33	0.23	38.01	46.44	0.06	0.69	0.88	7.50	3.12	2.79
River sand	0.22	0.12	4.04	91.67	0.03	0.02	2.08	0.24	0.87	0.53
Pumice stone	4.79	0.06	11.21	70.55	0.12	0.06	3.76	0.81	4.57	2.93

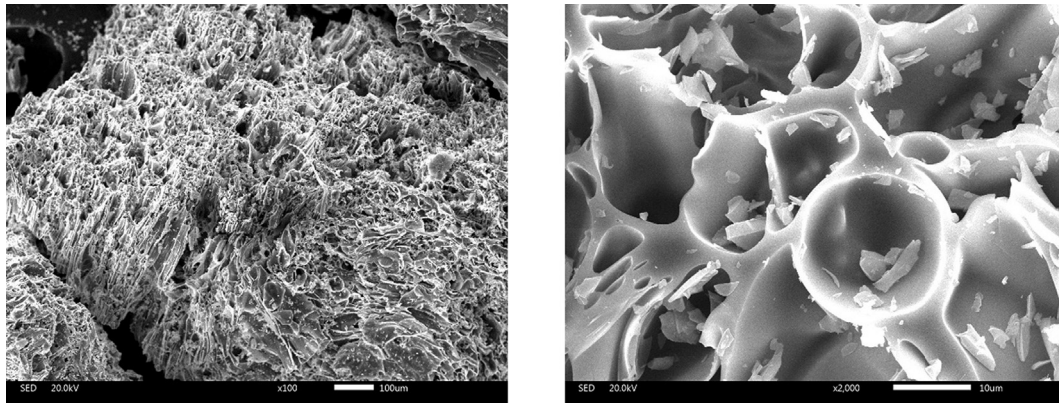


Fig. 1. SEM images of utilized pumice stone.

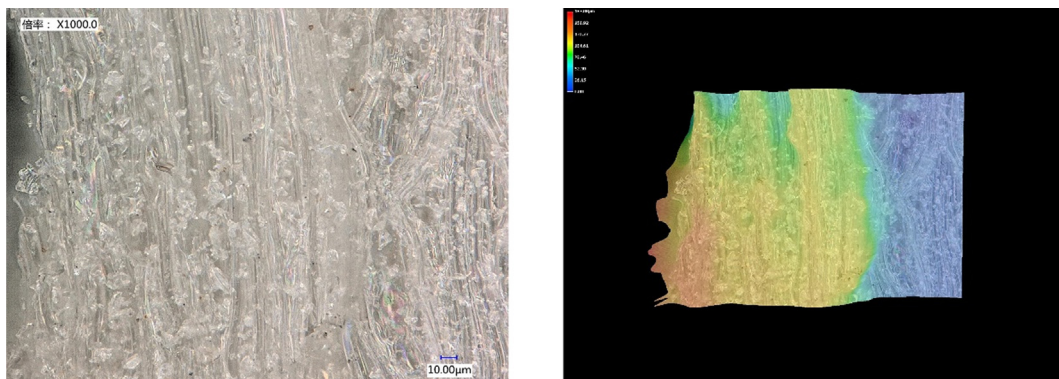


Fig. 2. 3D M pictures of employed pumice stone.

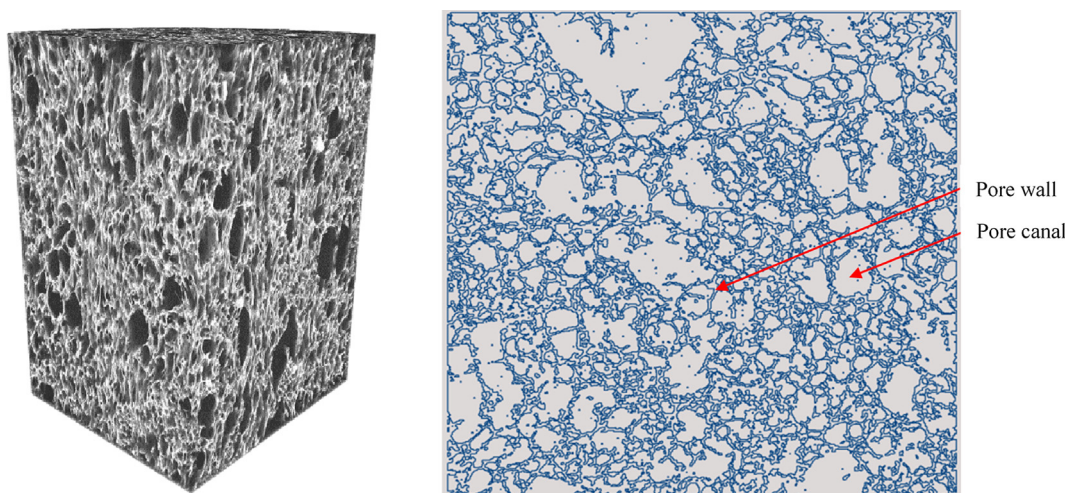


Fig. 3. CT photographs of used pumice stone.

The MIP characterization analysis of the natural pumice stone is displayed in Fig. 4. The obtained results show that the porosity of natural pumice is 51.6%, the main pore size distribution is 2–10 µm and the average pore diameter is 5.8 µm. This macro-porous structure can assure that the mortars or hydration products do not easily block the surface of the pores, causing the water release process to be interrupted. Furthermore, the capillary force action in the macro-pore is weak, which means the water is easy to release with a decrease of relative humidity (RH) in the exterior condition [50]. The BET – BJH analysis results of the fine aggregates of pumice with different particle sizes after crushing are provided in Fig. 5. The results reveal that the adsorption – desorption curves and BJH pore size distribution trends of the two kinds of pumices are similar to each other, manifesting that both types of pumice contain a certain amount of micro-pores and mesoporous structures. The peak of pore size distribution of pumice (0–0.6 mm) is significantly higher than that of pumice (0.6–1.25 mm), because the smaller the particle size, the larger the specific surface area, simultaneously, the more pore structures formed by the accumulation of granules [51]. The specific surface area, pore volume and average pore diameter of pumice (0–0.6 mm) and pumice (0.6–1.25 mm) are 0.93 m²/g and 0.59 m²/g, 2.6 × 10⁻³ cm³/g and 1.5 × 10⁻³ cm³/g, 11.30 nm and 10.22 nm, respectively. The micro-pores and mesoporous structure will also affect the behavior of water absorption – release of pumice particles [52].

The TG – DTG curves of pre-humid pumice (setting indicator: 15 °C–80 °C, 0.5 K/min) with different granule sizes under the surface dry condition are exhibited in Fig. 6. Based on the obtained experimental results, it can be summarized as follows: 1) The TG curves of pumice (0–0.6 mm) and pumice (0.6–1.25 mm) have similar laws, indicating that the adsorption of water by the pore structure of pumice with different pore size distribution mainly depends on capillary force action; 2) It can also be seen from the TG curves that the water absorption rate of pumice (0.6–1.25 mm) is faster than that of pumice (0–0.6 mm). This is due to the fact that part of the pore structure of pumice is destroyed during the crushing process, especially the macro-pores texture. Then, more macro-pores are generated in pumice (0.6–1.25 mm). Under the action of capillary force, the absorption-release process of pores follows the rule from macro-pores to micro-pores [53], consequently pumice (0.6–1.25 mm) has a higher water absorption rate than that of pumice (0–0.6 mm); 3) It can be observed that the initial water release rate of pumice (0–0.6 mm) and

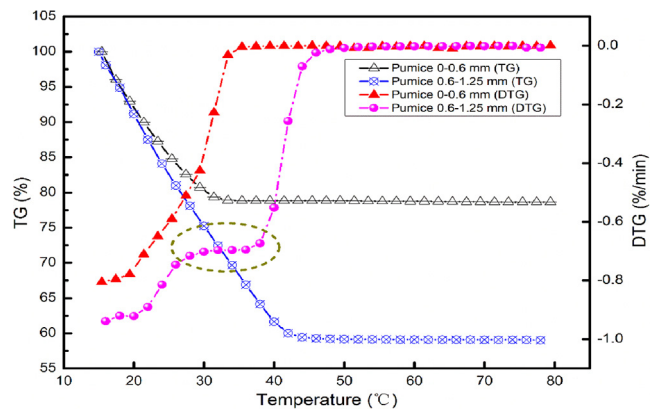


Fig. 6. TG – DTG curve of crushed pumice (0–0.6 mm) and pumice (0.6–1.25 mm).

pumice (0.6–1.25 mm) are similar to each other. Nevertheless, pumice (0.6–1.25 mm) has a distinct “locking-in water” process in the temperature range of 26 °C–38 °C. During this process, there may be a dynamic balance between the increase of kinetic energy of water molecule (caused by the increase of temperature in the pore channel) and the suction force under the action of capillary. With a further increase of temperature, the equilibrium relationship is broken, and the water release rate of pumice (0.6–1.25 mm) and pumice (0–0.6 mm) return to the same level. The characteristic of pumice (0.6–1.25 mm), which has unique “locking-in water” function, provides a possibility for the potential matching between the stage of periodic release process of pumice fine aggregates and the phase of “water requirement” when the internal RH inside concrete drops. It again can be predicted that the pumice (0.6–1.25 mm) as internal curing material has a greater internal curing efficiency. The saturated water absorption of pumice (0–0.6 mm) and pumice (0.6–1.25 mm) measured by the wet mark method is 77.9% and 66.6%, respectively, based on saturated surface dry method [54]. The apparent density of river sand (0–0.6 mm) and river sand (0.6–1.25 mm) by the standard method is 2.66 g/cm³ and 2.60 g/cm³, respectively, according to the JGJ 52–2006. The apparent density of pumice (0–0.6 mm) and pumice (0.6–1.25 mm) surveyed by the equal volume method is 40.6% and 22.7% of the same sized river sand, respectively.

2.2. Experimental methodology

2.2.1. UHPC mix design method

In this study, the modified Andreassen and Andersen (A&A) particle packing model is used to design the mix recipe of UHPC, in which the distribution modulus (q) takes a value of 0.23 [55–57]. Based on the modified (A&A) model, the designed actual curve and the target curve can be as close as possible by adjusting the proportion of particle size distribution of diverse cementitious materials and fine aggregates, to obtain the tightest packing state of the system. Then, the pumice with different water absorption rates, under unsaturated water absorption (19.0%) and saturated water absorption (77.9% or 66.6%) conditions, respectively, is utilized to replace river sand by 10%, 20% and 30%. Some detailed information for the UHPC recipe is shown in Tables 2 and 3, respectively. Owing to the fact that the mechanical strength of pumice itself is not as good as river sand, to avoid the UHPC strength decrease after including pumice, a more reasonable accumulation program should be adopted. According to a further adjustment of each individual materials, the optimized grading curve of the designed mixtures is posted in Fig. 7.

Table 2
Description of introducing pumice with different designed UHPC.

Group	Diameter (mm)	Admixture (vol. %)	Absorption (wt. %)	Extra water (kg/m ³)
E0	0	0	0	0
E1	0–0.6	10%	19.0%	5.9
E2		20%		11.8
E3		30%		17.7
E4	0.6–1.25	10%		0.96
E5		20%		1.92
E6		30%		2.88
E7	0–0.6	10%	77.9%	24.3
E8		20%		48.6
E9		30%		72.9
E10	0.6–1.25	10%	66.6%	3.35
E11		20%		6.7
E12		30%		10.05

Fig. 5. N₂-Sorption Isotherm curve and BJH pore size distribution of crushed pumice (0–0.6 mm) and pumice (0.6–1.25 mm).

Table 3Mix design of UHPC with different volume fraction of pumice (kg/m^3).

Group	Cement	FA	SF	River sand		Pre-wetting pumice		Water	SP
				0–0.6	0.6–1.25	0–0.6	0.6–1.25		
E0	750	200	144	770	220	0	0	175	31
E1				693	220	37.08	0		
E2				616	220	74.16	0		
E3				539	220	111.24	0		
E4				770	198	0	6.00		
E5				770	176	0	12.00		
E6				770	154	0	18.00		
E7				693	220	55.43	0		
E8				616	220	110.86	0		
E9				539	220	166.29	0		
E10				770	198	0	8.38		
E11				770	176	0	16.76		
E12				770	154	0	25.14		

2.2.2. Flowability test

After terminating of the mixing process, the flowability of fresh UHPC with different amount of pre-wetting pumice is evaluated based on the GB/T 2419-2005. The maximum diffusive diameters in 2–3 diverse directions of the bottom discoid mortar are measured, and the size of the diffusion diameters indicate the degree of fluidity.

2.2.3. Setting time test

After mixing, the setting time of the designed UHPC mixtures incorporating pre-wetting pumice are measured according to the GB/T 50080-2016. Under the test condition of $20 \pm 2^\circ\text{C}$, the initial setting time of mortar is confirmed when the required penetration resistance value per unit area reaches 3.5 MPa. Analogously, when the force value is 28 MPa, the corresponding time is the final setting time.

2.2.4. Mechanical properties test

The compressive strength of the designed UHPC is tested based on the GB/T 17671-1999. The fresh mortar is manufactured as standard specimen with the size of $40 \text{ mm} \times 40 \text{ mm} \times 160 \text{ mm}$, the compressive strength of 1 d, 7 d, 28 d and 56 d shall be measured, respectively, according to the specified method under standard curing conditions.

2.2.5. Autogenous shrinkage test

The autogenous shrinkage test is measured according to the GB/T 50082-2009. Adopting a $100 \text{ mm} \times 100 \text{ mm} \times 515 \text{ mm}$ prismatic specimen, the test mold is poured to 3/4 height after mixing, and the measurement is carried out under constant temperature of $20 \pm 2^\circ\text{C}$ and humidity of $60 \pm 5\%$. The final value of autogenous shrinkage is equal to the test value minus the amount of contraction before condensation.

2.2.6. Microstructure analysis

The impact of pre-wetting pumice addition on the microstructure development of the designed UHPC are appraised with several characterization means. The images analysis of ESEM, EBSD (Electron BackScattered Diffraction) and 3D M was used to evaluate the morphological features and compactness of ITZ between aggregates (river sand/pre-wetting pumice) and paste. The MIP plays a brilliant role in understanding the pore structure, including total porosity and pore size distribution of the hardened mixture. Meanwhile, the CT analysis is an auxiliary approach to visually estimate the fine microstructure characteristics of UHPC in a panoramic presentation fashion. Apparently, all the samples should be pretreated according to the requirements of relevant tests.

3. Results and discussions

3.1. Fresh behavior of the developed UHPC with porous pumice

The flowability of the designed UHPC with compounded pre-wetting pumice particles is shown in Fig. 8. It can be noticed that with an increase of the included pumice particles, the UHPC flowability simultaneously increase. For example, E0 is the reference group with a fluidity of 183 mm. When 20% or 30% river sand (0–0.6 mm) is replaced by pumice (0–0.6 mm), the UHPC flowability can be enhanced to 345 mm and 374 mm, respectively. This phenomenon should be attributed to the included free water amount by pumice. Based on the calculation, about 48.6 g and 72.9 g theoretical water are additionally included into the UHPC system by the carrier effect of pumice. These extra involved water can directly enhance the water to binder ratio of UHPC, and simultaneously increase its flowability. When the included theoretical water by pumice is relatively low (e.g. E11 and E12), the UHPC flowability is comparable (181 mm and 186 mm for E11 and E12, respectively) to the reference sample.

In addition, pumice (0.6–1.25 mm) has more obvious contribution of the UHPC flowability than that of pumice (0–0.6 mm). To be specific, E2 (20% pumice (0–0.6 mm)) brings 11.8 g water in UHPC mixture, but its fluidity decreases by 5.5% compared with the reference group. Contrastively, E6 (30% pumice (0.6–1.25 mm)) introduces 2.9 g water into the system, and it increases by 9.8% matching E0 in flowability. This phenomenon is due to there is a dynamic balance between the synergistic effect of water-absorbent pumice on the “water-releasing” and “water-absorbing” behavior in paste during the course of mixing, and the “water-absorbing” rate is much faster than that of “water-releasing”. For both E2 and E6 in the condition of unsaturated water absorption of pumice, pumice (0–0.6 mm) has a higher

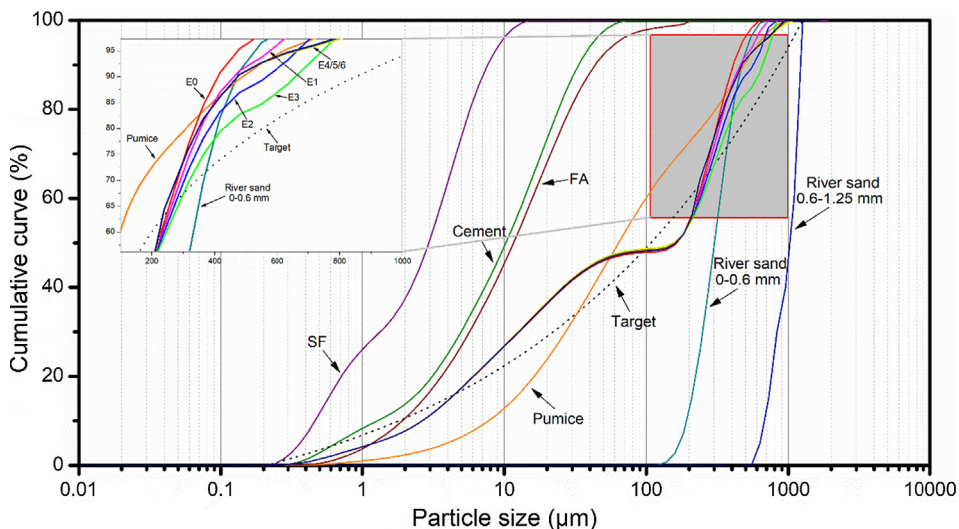


Fig. 7. Particle size distributions (PSDs) of the raw materials, the target and optimized grading curves of UHPC with different volume fraction of pumice.

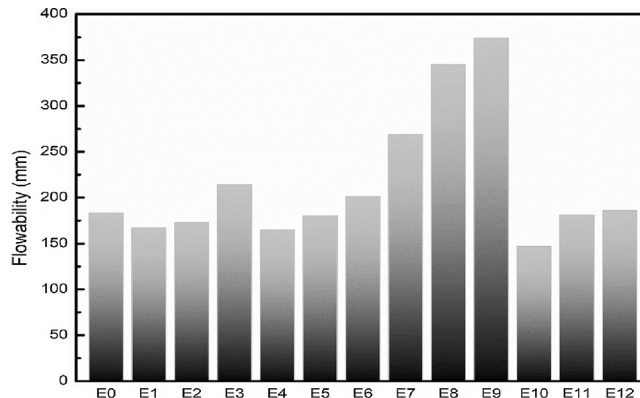


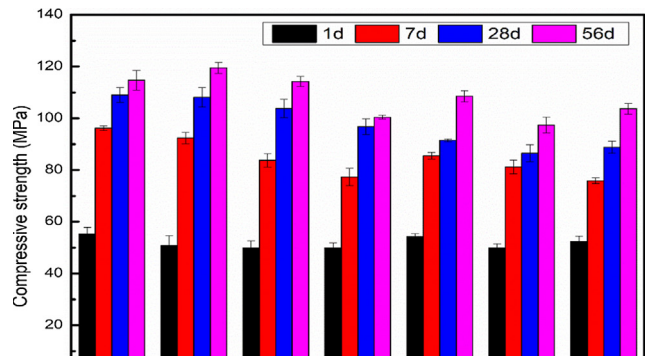
Fig. 8. The flowability of the designed UHPC with compounded pre-wetting pumice.

specific surface area and a lower proportion of macropores, and its “water-absorbing” behavior predominates, resulting in a reduction of water involved in the UHPC mixing. Nevertheless, pumice (0.6–1.25 mm) takes an opposite property in terms of specific surface area and proportion of macro-pores, which leads to the increase of water in the mixing process and enhances the working performance under the function of rotor centrifugal force.

The setting times of the UHPC system prepared with different pumice proportions are given in Fig. 9. It is clear that the variation law of setting time is basically consistent with the overall rule of working performance, which is determined by the diversity of the total amount of water introduced and the water release behavior of pumice particles with different sizes. The change trend of initial setting time and final setting time curves agree well, and the initial setting time is set as “Time Zero” in the subsequent evaluation of autogenous shrinkage characteristics.

3.2. Mechanical properties of the developed UHPC with porous pumice

The effect of pre-wetting pumice on the compressive strength of UHPC is presented in Fig. 10. It is important to find that the introduction of aquiferous pumice can inhibit the early strength development of UHPC as a whole, but there is an obvious compensation strength development effect after 28 days. Their overall strength at 56 d approaches or exceeds the reference group, which can well meet the requirements of UHPC on the strength index. For instance, the early strength of all the developed UHPC mixtures is smaller than that of reference sample by 5–20% at 7 d. When the curing time is extended to 56 days, the compressive strength of



(a) E1-E6

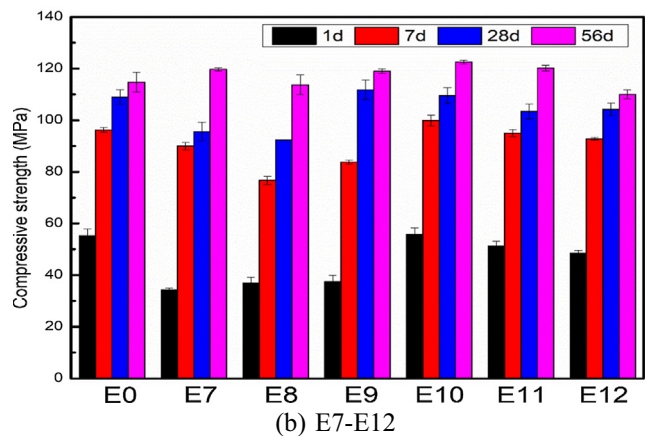


Fig. 10. Influence of the hydrous pumice on the compressive strength development of the designed UHPC at 1 d, 7 d, 28 d and 56 d.

all the UHPC specimen is comparable or even higher than the reference sample. To explain the phenomenon mentioned above, the involved extra water should be focused. In general, the moisture introduced by the pre-wetting pumice has two effects on UHPC system: deteriorating hydration products and promoting hydration process. In the early stage of hydration, the influence of mechanical properties is dominated by the exacerbating effect. The water brought into the UHPC system by the hydrous pumice leads to an increase in the actual water-binder ratio (w/b), which in turn affects the structure of hydration products, resulting in a strength landslide [58]. Correspondingly, in the later period, the water released from the pumice further promotes the continued hydration of a large number of unhydrated cement particles and secondary hydration of SF and FA active powders internally, thereby achieving the function of compensating the development of strength in the later hydration course.

The intensity of natural pumice stone is relatively low, but there is no strength collapse for the developed UHPC in this study. The reasons can be generalized as follows: 1) Extra water to participate in hydration, which can improve the hydration degree of cementitious materials, and optimize the pore structure and ITZ framework within UHPC; 2) In the process of crushing natural pumice into desired size particles, with the destruction of pore structure, the internal defects decrease, resulting in a change in the form of failure mode, and the intensity of the particles own are reinforced [59]; 3) The chief origin of ultra-high strength for UHPC is the tightest stacking effect between granules. Under the situation that the accumulation model is not evident deteriorated, its mechanical properties can be well protected [60].

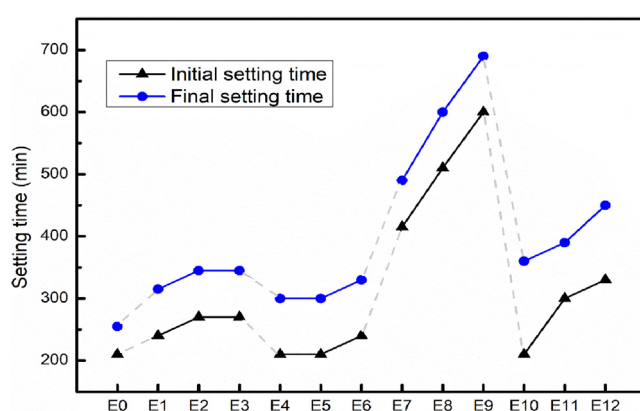


Fig. 9. The setting times of the UHPC mixtures prepared with different mixing proportions.

3.3. Autogenous shrinkage of the developed UHPC with porous pumice

The autogenous shrinkage of UHPC mixtures with different content of hydrous pumice is illustrated in Fig. 11. As can be gotten, the autogenous deformation evolution of UHPC can be divided into three phases: rapid growth, callback and moderate growth. These three stages are closely related to a series of physical and chemical reactions in the process of hydration [61]. The rapid growth progress of self - deformation is mainly concentrated within 12 h after initial condensation, and the contraction quantity reaches more than 40% of the total amount of autogenous shrinkage in 7 d. The autogenous deformation development characteristic at this stage is the key factor to determine the volume stability of concrete. Under the condition that the introduced water is controlled at a lower level, the amount of contraction in the self - shrinkage rapid growth stage can be extremely limited, which contributes strikingly to the shrinkage-reducing effect of the system. The gradual rise period of autogenous shrinkage gives expression to the continuous evolution process and predictable prospect for the later development. The introduction of water will obviously cut down the rate of autogenous deformation pullulation in the gentle growth phase. Regardless of the amount of water brought in, the curves of different substitution systems in the moderate growth stage will eventually tend to be parallel, and the rate of deformation will return to the similar level. The manifestation of the self - contracting evolvement of UHPC system is closely bound up with the degree of internal RH decline [62–64]. As internal curing material, moisture released from pre-wetting pumice particles will greatly delay the self-desiccation phenomenon inside UHPC, which

is perfectly reflected in the rapid and moderate growth of the autogenous shrinkage evolution curves.

In this study, the water intake of pumice is the crux to decide its internal curing effect. Within an appropriate range (less than 17.7 g of extra theoretical water), the pre-wetting pumice has a notable internal curing consequence. Nevertheless, when the theoretical extra water content is relatively high (more than 24.3 g), a notable negative effect on UHPC constriction development could be found. To be specific, the reference sample has an autogenous shrinkage of $733 \mu\epsilon$, which could be reduced by 30–50% with an addition of hydrous pumice. However, E7–E9 shows a very slight degree of contraction reducing, even a phenomenon of increased autogenous deformation, which is related to the constriction amplification within the phase of rapid growth process. The intrinsic reason is that there is more extra water brought in UHPC system, resulting mutations in hydration products and microstructure evolution, which will inhibit the strength development within first 12 h. Sufficient hydration accelerates the growth of autogenous shrinkage [65], meanwhile, the strong slide of mechanical properties will seriously weaken the restraining action on the enlarge of contraction deformation, leading to the ultimate shrinkage-reducing effect is not obvious and indeed an increase.

In summary, based on these obtained experimental results (as fresh behavior, mechanical properties and autogenous shrinking development), it can be concluded that the UHPC incorporating with 0.6–1.25 mm graded pumice particles has a better comprehensive capability in producing advanced UHPC. Taking E12 as an example, its fluidity is 186 mm, the initial setting time is 330 min, the 28 d compressive strength is 104.2 MPa, and the 7d autogenous deformation is $363 \mu\epsilon$. Finally, the fresh and hardened state density of samples are exhibited in Table 4.

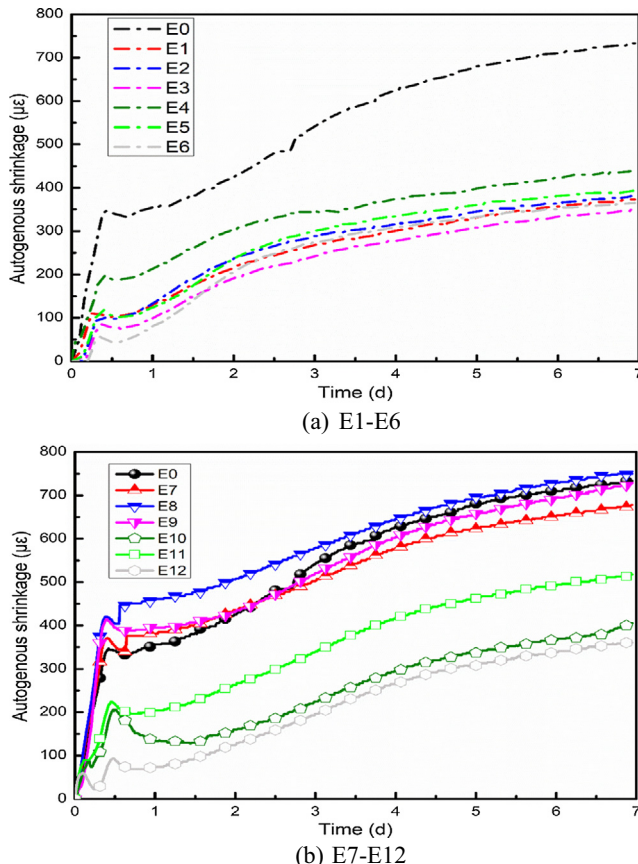


Fig. 11. The autogenous shrinkage of UHPC mortar with different content of aquiferous pumice.

3.4. Pore structure of the developed UHPC with porous pumice

3.4.1. Characterization of MIP

The standard curves of pore size structure and cumulative porosity of the developed UHPC with different amount of hydrous pumice after curing for 7d and 28d are illustrated in Figs. 12 and 13. The results of pore size distribution and cumulative porosity obtained by MIP characterization actually reflect the composite system of UHPC matrix and pumice aggregates, including the pore parameter information of pumice itself and concrete. Through the combined analysis of BJH on pumice particles with disparate sizes and MIP data of concrete composites, the pore parameters of the part introduced by pumice beads are peeled off. It is found that the numerical value of pore structure corresponding to MIP in the range of 1–100 nm is more than 5 orders of magnitude higher than that of BJH data. Therefore, it can be considered that the

Table 4
Fresh and hardened state density of designed UHPC samples (kg/m^3).

Group	Density	
	Fresh state	Hardened state
E0	2290	2271
E1	2250	2226
E2	2210	2179
E3	2170	2132
E4	2274	2253
E5	2258	2232
E6	2242	2213
E7	2268	2239
E8	2247	2211
E9	2225	2180
E10	2276	2255
E11	2263	2236
E12	2249	2218

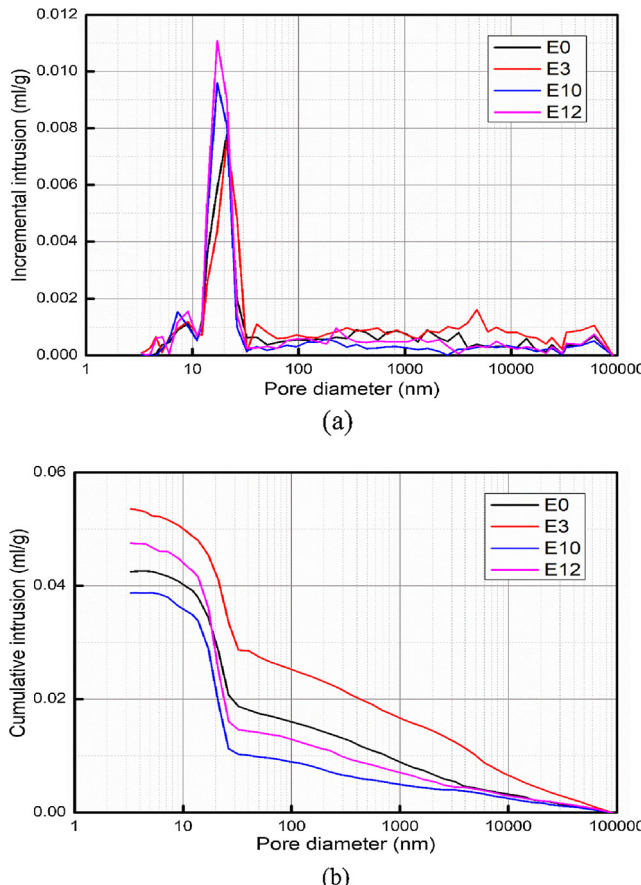


Fig. 12. Pore structure analysis of several typical UHPC mixtures after curing for 7 days: (a) incremental intrusion; (b) cumulative intrusion.

curves given by MIP represent the pore structure characteristics of UHPC paste.

Based on the information shown in Fig. 12, it is clear that the incorporation of bibulous pumice has a visible impact on the pore size distribution and porosity of UHPC system. Some detailed values are summarized in Table 5. Compared with E0, the average diameter and most probable pore size of E10 and E12 drop clearly, while the capillary volume fraction palpably raised. At the same time, the opposite characteristic changes occur in E3. It indicates that the mixing of hydrous pumice with larger particle size can refine the capillary pore of concrete, while the minor sized pumice has a detrimental effect. This is due to the remarkable furtherance on hydration of pumice (0.6–1.25 mm), while the water release proceeding of pumice (0–0.6 mm) is extremely inhibited. The former generates more hydration products, which will fill part of the large pores, reducing the average diameter of capillary pore and elevating the pore capacity [66]. Capillary characteristics have little effect on strength of concrete [67], nevertheless, they are closely related to autogenous shrinkage and deformation. Relevant studies have shown that capillary pores of 5–50 nm are the main region of autogenous shrinkage in conventional UHPC system, and there is a well positive linear relationship between them [68]. In this study, the ordinance is equally followed under the internal curing mechanism. However, incorporating E0 into the comparison frame, that rule will be broken. The interrelation between each group on capillary fraction is E10 > E12 > E0 > E3, a quite distinct trend in corresponding value of autogenous shrinkage presents a nexus exactly as E0 (733 $\mu\epsilon$) > E10 (405 $\mu\epsilon$) > E12 (363 $\mu\epsilon$) > E3 (349 $\mu\epsilon$). This manifestation can be attributed to the germination and evolution of meniscus curvature and surface tension within capillary pores [69]. Under the surrounding of

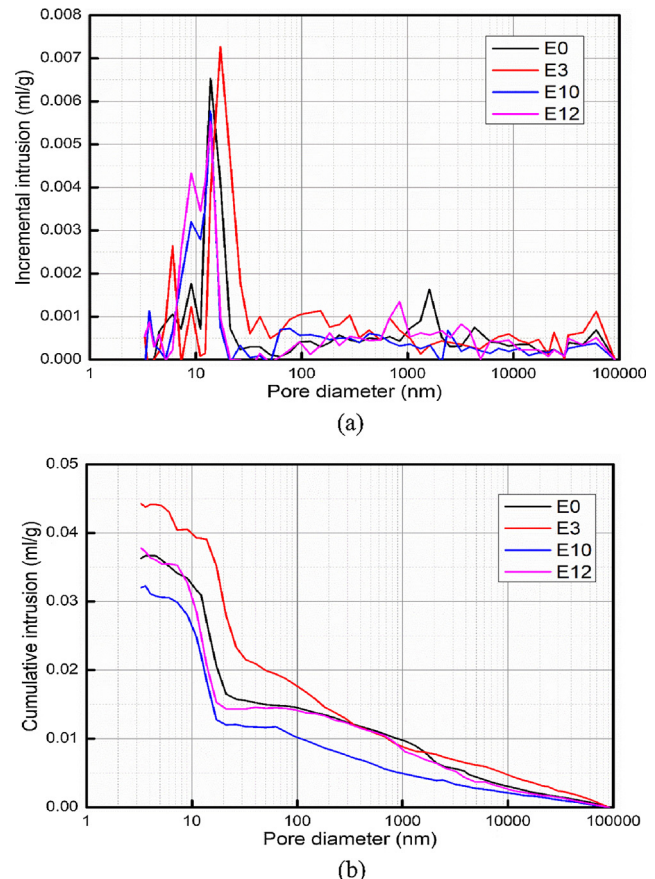


Fig. 13. Pore structure analysis of several typical UHPC mixtures after curing for 28 days: (a) incremental intrusion; (b) cumulative intrusion.

Table 5

Details of pore characteristics of representative formulations at 7 d age.

Sample code	E0	E3	E10	E12
Total porosity (%)	9.1	10.9	8.2	9.8
Coarse fraction (%)	48.2	56.3	33.8	37.5
Capillary fraction (%)	51.8	43.7	66.2	62.5
Average diameter (nm)	32.4	34.9	24.7	24.8
Most probable pore size (nm)	21.1	21.1	17.1	17.1

“water-rich”, the speed and degree of capillary negative pressure increase are strikingly lower than that in the condition of “seal”, causing the self-desiccation effect is slowed down accordingly. Furthermore, the variation tendency of total porosity in different recipes and the performance of compressive strength as mentioned in previous paper, embodied as E10 (99.9 MPa) > E0 (96.2 MPa) > E12 (92.8 MPa) > E3 (77.3 MPa), are well verified.

The index of average diameter, most probable pore size and total porosity of each group at 28 d has similar regularity with that of 7 d, which is detailed presented in Table 6. The notes display

Table 6

Details of pore characteristics of representative formulations at 28 d age.

Sample code	E0	E3	E10	E12
Total porosity (%)	8.2	9.3	7.2	7.7
Coarse fraction (%)	51.5	54.4	46.6	43.7
Capillary fraction (%)	48.5	45.6	53.4	56.3
Average diameter (nm)	26.4	30.2	19.4	17.4
Most probable pore size (nm)	13.7	17.1	13.7	13.7

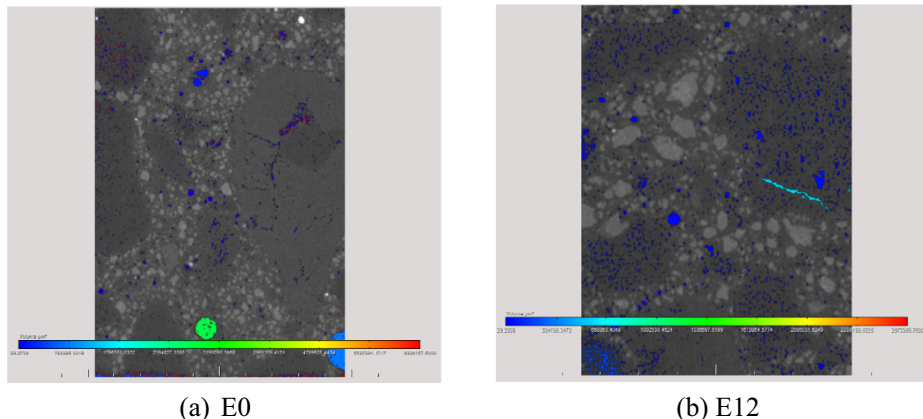


Fig. 14. The representative CT images of E0 and E12 specimens after 7 d curing.

that with the increase of curing age, the degree of pore structure refinement of every sample is risen to a certain extent, and the total porosity is further reduced. Compared with the specimens at 7 d, the corresponding most probable pore size of E0, E3, E10 and E12 decreases by 34.9%, 18.9%, 19.7% and 19.7%, respectively; The average diameter reduces by 18.5%, 13.5%, 21.5% and 29.8%, respectively; The total porosity drops by 9.6%, 14.4%, 12.4% and 21.5%, respectively; The capillary fraction slides by 6.4%, -4.3%, 19.3% and 9.9%, respectively.

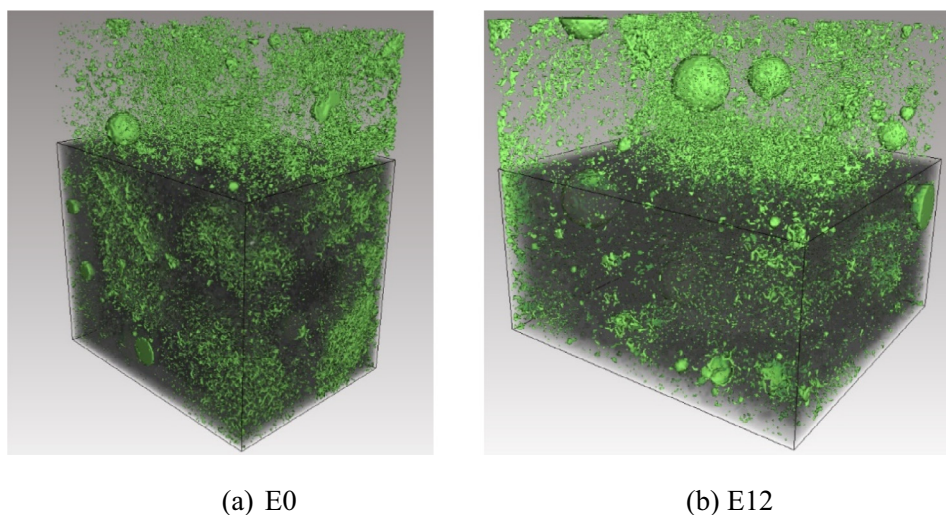
By contrastive analysis with the absolute value of the homologous data, it can be achieved that under the condition of brilliant internal curing effect, the pore structure of later period of UHPC system could be deteriorated by adding hydrous pumice (0–0.6 mm), while pumice (0.6–1.25 mm) can optimize the porous framework, which is consistent with the macro performance.

3.4.2. Characterization of CT

Considering the fact that there are some limitations on the characterization of concrete pore structure by MIP, which can only reflect the characteristics of connected pores, the closed pores should also be evaluated based on other techniques. CT is a method that could comprehensively evaluate the communicating and sealing holes, which is an available auxiliary method to investigate pore structure in concrete.

Here, the representative CT images of E0 and E12 specimens after 7 days curing is exhibited in Fig. 14, meanwhile, the parameters of the two types of pores and their scales are exposed in Table 7. It can be discovered that at 7 d, the total porosity of E12 is higher than that of E0, which is identical with the result of MIP expression. The volume fraction of connected pores in E0 and E12 is 37.0% and 61.4%, respectively. Interlocking pores are channels for moisture migration and material diffusion [70]. The proportion of intercommunicating

Parameters (%)		E0	E12
Porosity	Total porosity	6.84	8.17
	Non-connected porosity	4.31	3.15
Scale and quantity	Connected porosity	2.53	5.02
	Amount (3–100 μm^3)	92.88	89.60
	Volume (3–100 μm^3)	48.53	40.26
	Amount (100–1000 μm^3)	6.85	9.91
	Volume (100–1000 μm^3)	20.46	28.43
	Amount (1000–1 \times 10 ⁴ μm^3)	0.24	0.47
	Volume (1000–1 \times 10 ⁴ μm^3)	8.50	12.71
	Amount (1 \times 10 ⁴ –8 \times 10 ⁵ μm^3)	0.023	0.025
	Volume (1 \times 10 ⁴ –8 \times 10 ⁵ μm^3)	22.51	18.60



Green indicator: Pore; Grey indicator: Mortar

Fig. 15. The CT 3D model of holes framework features of E0 and E12 samples.

pores in E12 is overtly advanced, which is mostly attributed to two aspects: 1) Primary cause is that the extra water introduced by pumice “tank” will leave a series of potential connected holes in the transfer route during the sustained release process in the slurry; 2) The abundant connected pores structure of pumice itself also contribute to the enlargement of patulous apertures. The features of micron level coarse holes in concrete are mainly determined by the packing form, vibrating technology and flowability [71,72]. In this study, UHPC mixtures E0 and E12 have very similar casting process and flowability. Nevertheless, the amount and volume fraction of the minimum scale holes ($3\text{--}100 \mu\text{m}^3$) visible by CT in E12 is slightly lower than that of E0. It is proved that the stacking state of UHPC blended with pumice containing water is infinitesimally

degenerated, which is caused by the multi edge angle shape of the crushed pumice stone [73]. The holes framework features of E0 and E12 are also intuitively reflected in the CT 3D model, as presented in Fig. 15.

3.5. Microstructure development and ITZ analysis

It is universally known that ITZ, as a weak link, has a major negative impact on the homogeneity of concrete, especially the overall mechanical properties and durability [74]. The morphological characteristics of ITZ between the fine aggregates and paste in hardened UHPC as defined earlier are demonstrated in Figs. 16–18. Comparing to the river sand, the ITZ framework formed

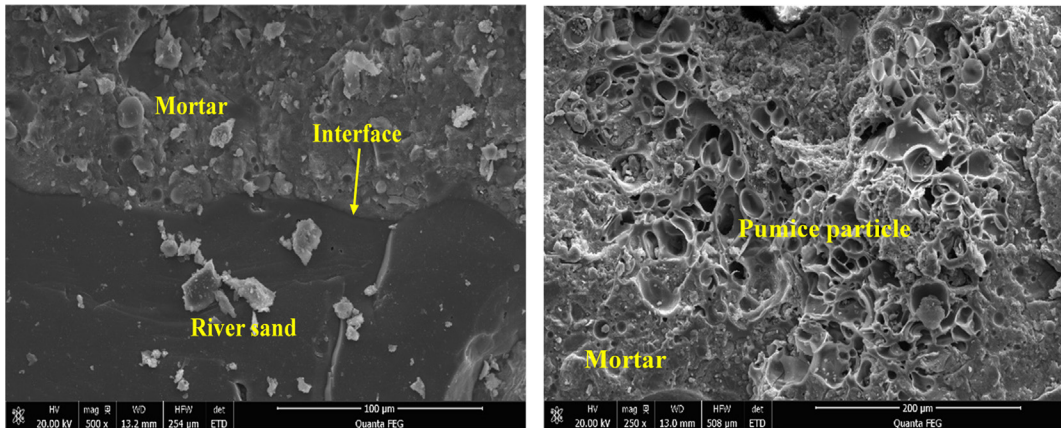


Fig. 16. The ESEM pictures of ITZ framework formed between hydrous pumice/river sand and UHPC matrix.

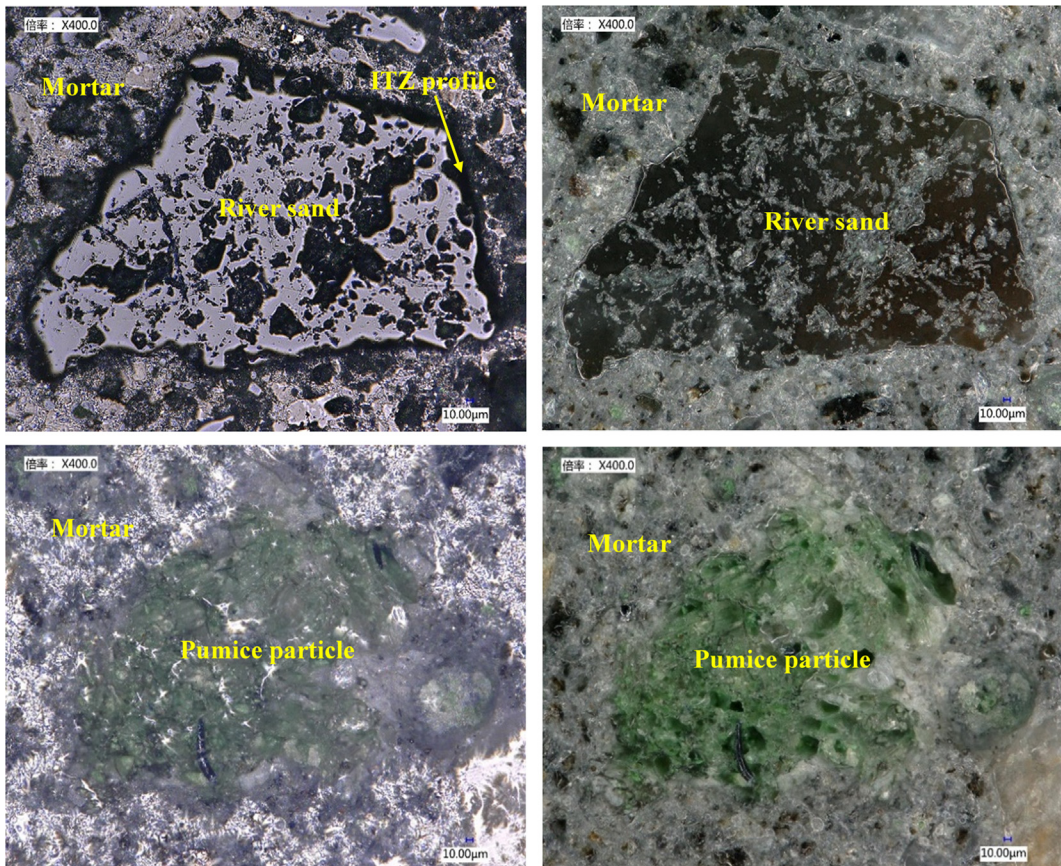


Fig. 17. The appearance of ITZ of retrospective double fine aggregates and mortar under 3D M polarization.

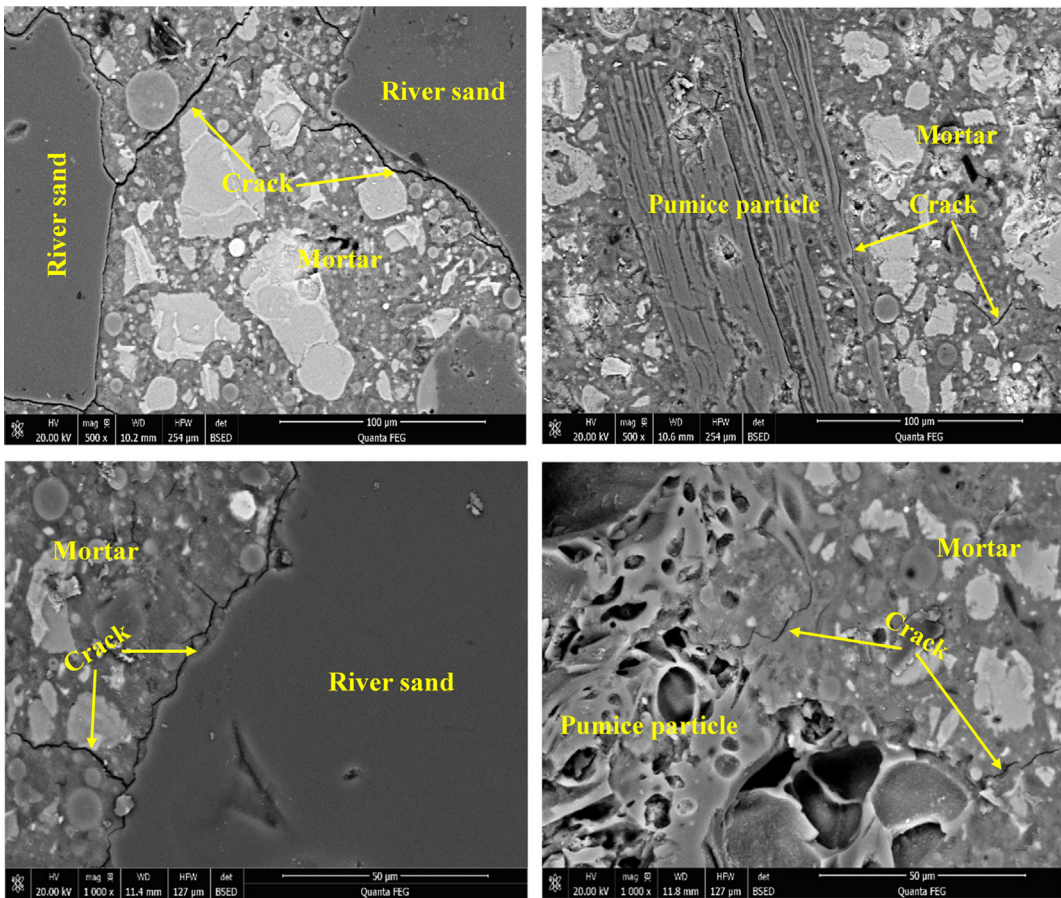


Fig. 18. EBSD photographs of ITZ previous mentioned double fine aggregates and paste.

between hydrous pumice and UHPC paste is obviously optimized - narrowed and densified. Fig. 16 shows the ESEM images of ITZ between river sand / pre-wetting pumice and paste of E12 specimen at 28 d. It is clear that the ITZ boundary between river sand and mortar is obviously visible, while the ITZ structure of aquiferous pumice – UHPC paste do not show significant borderline and contour. The appearance of ITZ of retrospective double fine aggregates and mortar is exhibited under 3D M polarization in Fig. 17. Stick out a mile, the width of the ITZ architecture between hydrous pumice particles and UHPC paste is much narrower than that of river sand. Fig. 18 displays the EBSD photographs of ITZ previous mentioned, which can be noticed is that under the action of external physical friction, the cracks are more likely to grow and propagate at ITZ of river sand – UHPC paste, while the degree of damage to the ITZ of water-absorbing pumice – UHPC paste is seriously eliminated. This is attributed to that the moisture discharged from the aquiferous pumice can promote the hydration of the reaction layer of ITZ, and improve the overall hydration degree of ITZ structure, thus achieve the purpose of optimizing the ITZ framework [75].

Furthermore, the hydration products generated in the ITZ region, such as AFt, Ca(OH)₂ and C-S-H, can grow in the pore passages of pumice after water release, increasing the meshing effect of the interface, just as "wedges" to reinforce the entire ITZ structure. Meanwhile, the oriented growth of Ca(OH)₂ has also been restrained to a certain extent, which further promotes the compaction of ITZ [76]. Narrowing and densification of ITZ between fine aggregate and mortar is also an important source of mechanical performance enhancement for the UHPC system incorporating hydrous pumice.

4. Conclusions

In this paper, the hydrous pumice is utilized to produce UHPC, and its effect on the autogenous shrinkage and microstructure development of the developed UHPC are studied. Based on the obtained experimental results and comprehensive characterization analysis, the conclusions are summarized as follows:

- (1) The flowability of fresh UHPC incorporating pre-wetting pumice is determined by whether the pumice "tank" extract or inject free water to the system during the mixing process. For the pumice (0–0.6 mm), the included extra water is relatively less, and the extraction effect is dominant. In contrary, for pumice (0.6–1.25 mm), the volume substitution fraction is more than 20%, and the injection action comes into prominence.
- (2) The introduction of hydrous pumice does not cause the collapse of mechanical properties of UHPC. Wet pumice will inhibit the strength development of UHPC in the first 7 days as a whole, however, there is an obvious compensatory intensity development effect after 28 d, and the average compressive strength of 56 d can reach 98.0% of the reference group.
- (3) Water intake of pumice is the key factor in determining the efficiency of internal curing. The content of extra water is less than 17.7 g, the pre-moistened pumice has a remarkable compressed contraction consequence, and the maximum amount of shrinkage deformation within 7 d can be reduced by 52.4%. Nevertheless, excessive quantities of water are introduced, the effect of shrinkage-reducing is extremely

- inconspicuous, and even the phenomenon of contraction increases. Furthermore, pumice particles with a high proportion of macro-pores have better potential internal curing effect.
- (4) The addition of pumice (0.6–1.25 mm) can refine the pore structure of UHPC, while that the pumice (0–0.6 mm) has completely opposite results. With an increase of curing time, the evolution characteristics of this pore structure are more prominent. Meanwhile, the fraction of interconnected pores in concrete will be raised by employing humid pumice aggregates, and the micron-sized pore distribution generated by accumulation is slightly degraded.
- (5) Compared with the ITZ between river sand and UHPC paste, the ITZ skeleton between hydrous pumice and mortar is clearly narrowed and densified.

Conflicts of interest

There is no conflict of interest in this paper.

Acknowledgements

The authors acknowledge the financial supports of National Nature Science Foundation Project of China (51608409), Major science and technology project in Zhongshan city, Guangdong province (2017A1021), Yang Fan plan of Guangdong Province (201312C12), Science and Technology Program of Guangdong Province in 2016 (2016A090924002), Science and Technology Program of Guangdong Province in 2017 (2017B090907009), Late-model Research Institute Development Program of Zhongshan in 2016: Subsidy for Major Research Platform Construction (2016F2FC0008), and open research project of Advanced Engineering Technology Research Institute of Wuhan University of technology in Zhongshan city (WUT201802).

References

- [1] P. Richard, M. Cheyrezy, Composition of reactive powder concretes, *Cem. Concr. Res.* 25 (7) (1995) 1501–1511.
- [2] R. Yu, Development of Sustainable Protective Ultra-High Performance Fibre Reinforced Concrete (UHPFRC): Design, assessment and modeling PhD thesis, Eindhoven University of Technology, Eindhoven, the Netherlands, 2015.
- [3] C. Shi, Z. Wu, J. Xiao, et al., A review on ultra high performance concrete: Part I. Raw materials and mixture design, *Constr. Build. Mater.* 101 (2015) 741–751.
- [4] D. Wang, C. Shi, Z. Wu, et al., A review on ultra high performance concrete: Part II. Hydration, microstructure and properties, *Constr. Build. Mater.* 96 (2015) 368–377.
- [5] M.H. Zhang, C.T. Tam, M.P. Leow, Effect of water-to-cementitious materials ratio and silica fume on the autogenous shrinkage of concrete, *Cem. Concr. Res.* 33 (10) (2003) 1687–1694.
- [6] K. Koh, G. Ryu, S. Kang, et al., Shrinkage properties of Ultra-High Performance Concrete (UHPC), *Adv. Sci. Lett.* 4 (3) (2011) 948–952.
- [7] A.M. Soliman, M.L. Nehdi, Effect of drying conditions on autogenous shrinkage in ultra-high performance concrete at early-age, *Mater. Struct.* 44 (5) (2011) 879–899.
- [8] V.Y. Garas, L.F. Kahn, K.E. Kurtis, Short-term tensile creep and shrinkage of ultra-high performance concrete, *Cem. Concr. Comp.* 31 (3) (2009) 147–152.
- [9] Pietro Lura, Ole Mejlhede Jensen, Klaas van Breugel, Autogenous shrinkage in high-performance cement paste: an evaluation of basic mechanisms, *Cem. Concr. Res.* 33 (2) (2003) 223–232.
- [10] I. Burkart, H.S. Müller, Creep and shrinkage characteristics of ultra high strength concrete (UHPC), in: Proceedings of the Second International Symposium on Ultra High Performance Concrete, Kassel University Press, Kassel, Germany, 2008.
- [11] T. Xie, C. Fang, M.S.M. Ali, et al., Characterizations of autogenous and drying shrinkage of ultra-high performance concrete (UHPC): an experimental study, *Cem. Concr. Comp.* 91 (2018) 156–173.
- [12] Y. Akkaya, C. Ouyang, S.P. Shah, Effect of supplementary cementitious materials on shrinkage and crack development in concrete, *Cem. Concr. Comp.* 29 (2) (2007) 117–123.
- [13] J.J. Park, S.W. Kim, G.S. Ryu, et al., The influence of chemical admixtures on the autogenous shrinkage ultra-high performance concrete, *Key Eng. Mater.* 452–453 (2011) 725–728.
- [14] M.S. Meddad, A. Taghit-Hamou, Pore structure of concrete with mineral admixtures and its effect on self-desiccation shrinkage, *ACI Mater. J.* 106 (3) (2009) 241–250.
- [15] A.M. Soliman, M.L. Nehdi, Effect of partially hydrated cementitious materials and superabsorbent polymer on early-age shrinkage of UHPC, *Constr. Build. Mater.* 41 (41) (2013) 270–275.
- [16] E. Ghafari, S.A. Ghahari, H. Costa, et al., Effect of supplementary cementitious materials on autogenous shrinkage of ultra-high performance concrete, *Constr. Build. Mater.* 127 (2016) 43–48.
- [17] W. Sun, H. Chen, X. Luo, et al., The effect of hybrid fibers and expansive agent on the shrinkage and permeability of high-performance concrete, *Cem. Concr. Res.* 31 (4) (2001) 595–601.
- [18] V. Corinaldesi, A. Nardinocchi, J. Donnini, The influence of expansive agent on the performance of fibre reinforced cement-based composites, *Constr. Build. Mater.* 91 (2015) 171–179.
- [19] D.Y. Yoo, N. Banthia, Y.S. Yoon, Effectiveness of shrinkage-reducing admixture in reducing autogenous shrinkage stress of ultra-high-performance fiber-reinforced concrete, *Cem. Concr. Comp.* 64 (2015) 27–36.
- [20] A.M. Soliman, M.L. Nehdi, Effects of shrinkage reducing admixture and wollastonite microfiber on early-age behavior of ultra-high performance concrete, *Cem. Concr. Comp.* 46 (4) (2014) 81–89.
- [21] D.Y. Yoo, S.W. Kim, Y.S. Yoon, et al., Benefits of using expansive and shrinkage-reducing agents in UHPC for volume stability, *Mag. Concr. Res.* 66 (14) (2014) 745–750.
- [22] L. Wu, N. Farzadnia, C. Shi, et al., Autogenous shrinkage of high performance concrete: a review, *Constr. Build. Mater.* 149 (2017) 62–75.
- [23] H.R. Pakravan, M. Latifi, M. Jamshidi, Hybrid short fiber reinforcement system in concrete: a review, *Constr. Build. Mater.* 142 (2017) 280–294.
- [24] W. Li, Z. Huang, G. Hu, et al., Early-age shrinkage development of ultra-high-performance concrete under heat curing treatment, *Constr. Build. Mater.* 131 (2017) 767–774.
- [25] D.Y. Yoo, S. Kim, M.J. Kim, Comparative shrinkage behavior of ultra-high-performance fiber-reinforced concrete under ambient and heat curing conditions, *Constr. Build. Mater.* 162 (2018) 406–419.
- [26] P. Shen, L. Lu, Y. He, et al., Experimental investigation on the autogenous shrinkage of steam cured ultra-high performance concrete, *Constr. Build. Mater.* 162 (2018) 512–522.
- [27] S.H. Kang, S.G. Hong, J. Moon, Shrinkage characteristics of heat-treated ultra-high performance concrete and its mitigation using superabsorbent polymer based internal curing method, *Cem. Concr. Comp.* 89 (2018) 130–138.
- [28] B. Craeye, M. Geirnaert, G.D. Schutter, Super absorbing polymers as an internal curing agent for mitigation of early-age cracking of high-performance concrete bridge decks, *Constr. Build. Mater.* 25 (1) (2011) 1–13.
- [29] V. Mechcherine, M. Gorges, C. Schroefl, et al., Effect of internal curing by using superabsorbent polymers (SAP) on autogenous shrinkage and other properties of a high-performance fine-grained concrete: results of a RILEM round-robin test, *Mater. Struct.* 47 (3) (2014) 541–562.
- [30] J. Justs, M. Wyrzykowski, D. Bajare, et al., Internal curing by superabsorbent polymers in ultra-high performance concrete, *Cem. Concr. Res.* 76 (2015) 82–90.
- [31] G.R.D. Sensale, A.F. Goncalves, Effects of fine LWA and SAP as internal water curing agents, *Int. J. Concr. Struct. Mater.* 8 (3) (2014) 229–238.
- [32] G.R.D. Sensale, A.B. Ribeiro, A. Goncalves, Effects of RHA on autogenous shrinkage of Portland cement pastes, *Cem Concr Comp* 30 (10) (2008) 892–897.
- [33] N.V. Tuan, G. Ye, K.V. Breugel, et al., The study of using rice husk ash to produce ultra high performance concrete, *Constr. Build. Mater.* 25 (4) (2011) 2030–2035.
- [34] G. Ye, V.T. Nguyen, Mitigation of autogenous shrinkage of ultra-high performance concrete by rice husk ash, *J. Chin. Ceram. Soc.* 40 (2) (2012) 212–216.
- [35] V.T.A. Van, C. Rößler, D.D. Bui, et al., Rice husk ash as both pozzolanic admixture and internal curing agent in ultra-high performance concrete, *Cem. Concr. Comp.* 53 (10) (2014) 270–278.
- [36] J. Liu, Z. Ou, J. Mo, et al., Effectiveness of saturated coral aggregate and shrinkage reducing admixture on the autogenous shrinkage of ultrahigh performance concrete, *Adv. Mater. Sci. Eng.* 2017 (4) (2017) 1–11.
- [37] W. Meng, K. Khayat, Effects of saturated lightweight sand content on key characteristics of ultra-high-performance concrete, *Cem. Concr. Res.* 101 (2017) 46–54.
- [38] Y. Lv, H. Huang, G. Ye, et al., Autogenous shrinkage of zeolite cement pastes with low water-binder ratio, *Proceedings of the 14th International Congress on the Chemistry of Cement*, Ghent University Press, Beijing, China, 2015.
- [39] S. Zhutovsky, K. Kovler, A. Bentur, Efficiency of lightweight aggregates for internal curing of high strength concrete to eliminate autogenous shrinkage, *Mater. Struct.* 35 (2) (2002) 97–101.
- [40] S. Zhutovsky, K. Kovler, A. Bentur, Influence of cement paste matrix properties on the autogenous curing of high-performance concrete, *Cem Concr Comp* 26 (5) (2004) 499–507.
- [41] S. Zhutovsky, K. Kovler, Effect of internal curing on durability-related properties of high performance concrete, *Cem. Concr. Res.* 42 (1) (2012) 20–26.
- [42] P. Lura, D.P. Bentz, D.A. Lange, et al., Measurement of water transport from saturated pumice aggregates to hardening cement paste, *Mater. Struct.* 39 (9) (2006) 861–868.
- [43] B. Akcay, M.A. Tasdemir, Optimisation of using lightweight aggregates in mitigating autogenous deformation of concrete, *Constr. Build. Mater.* 23 (1) (2009) 353–363.

- [44] B. Akcay, M.A. Tasdemir, Effects of distribution of lightweight aggregates on internal curing of concrete, *Cem Concr Comp* 32 (8) (2010) 611–616.
- [45] N. Kabay, A.B. Kizilkanat, M.M. Tüfekçi, Effect of Prewetted pumice aggregate addition on concrete properties under different curing conditions, *Period. Polytech.-Civ.* 60 (1) (2015) 89–95.
- [46] G. Orsi, G. Gallo, G. Heiken, et al., A comprehensive study of pumice formation and dispersal: the Cretaceous Tephra of Ischia (Italy), *J. Volcanol. Geoth. Res.* 53 (1–4) (1992) 329–354.
- [47] C. Klug, K. Cashman, C. Bacon, Structure and physical characteristics of pumice from the climactic eruption of Mount Mazama (Crater Lake), Oregon, *Bull Volcanol.* 64 (7) (2002) 486–501.
- [48] K.M.A. Hossain, Properties of volcanic pumice based cement and lightweight concrete, *Cem. Concr. Res.* 34 (2) (2004) 283–291.
- [49] H. Binici, Effect of crushed ceramic and basaltic pumice as fine aggregates on concrete mortars properties, *Constr. Build. Mater.* 21 (6) (2007) 1191–1197.
- [50] D. Zou, K. Li, W. Li, et al., Effects of pore structure and water absorption on internal curing efficiency of porous aggregates, *Constr. Build. Mater.* 163 (2018) 949–959.
- [51] A.G. Yiotis, A.K. Stubos, A.G. Boudouvis, et al., Pore-network modeling of isothermal drying in porous media, *Transport Porous Med.* 58 (1–2) (2005) 63–86.
- [52] S. Ghouchian, M. Wyryzkowski, P. Lura, et al., An investigation on the use of zeolite aggregates for internal curing of concrete, *Constr. Build. Mater.* 40 (3) (2013) 135–144.
- [53] L. Su, D. Niu, D. Luo, Research status on water absorption and desorption properties of lightweight aggregate, *Bull. Chin. Ceram. Soc.* 37 (6) (2018) 1897–1902 (in Chinese).
- [54] ASTM Committee C09, C1761: Standard Specification for Lightweight Aggregate for Internal Curing of Concrete, ASTM, 2013.
- [55] G. Hüskens, A Multifunctional Design Approach for Sustainable Concrete with Application to Concrete Mass Products PhD thesis, Eindhoven University of Technology, Eindhoven, the Netherlands, 2010.
- [56] R. Yu, P. Spiesz, H.J.H. Brouwers, Mix design and properties assessment of Ultra-High Performance Fibre Reinforced Concrete (UHPFRC), *Cem. Concr. Res.* 56 (2014) 29–39.
- [57] X. Wang, R. Yu, Z. Shui, et al., Mix design and characteristics evaluation of an eco-friendly Ultra-High Performance Concrete incorporating recycled coral based materials, *J. Cleaner Prod.* 165 (2017) 70–80.
- [58] P.C. Aitcin, High performance concrete, CRC Press, Boca Raton, United States, 2011.
- [59] D. Sarı, A.G. Pasamehmetoglu, The effects of gradation and admixture on the pumice lightweight aggregate concrete, *Cem. Concr. Res.* 35 (5) (2005) 936–942.
- [60] F.D.L. Sedran, Optimization of ultra-high-performance concrete by the use of a packing model, *Cem. Concr. Res.* 24 (6) (1994) 997–1009.
- [61] E.I. Tazawa, S. Miyazawa, T. Kasai, Chemical shrinkage and autogenous shrinkage of hydrating cement paste, *Cem. Concr. Res.* 25 (2) (1995) 288–292.
- [62] A. Loukili, A. Khelidj, P. Richard, Hydration kinetics, change of relative humidity, and autogenous shrinkage of ultra-high-strength concrete, *Cem. Concr. Res.* 29 (4) (1999) 577–584.
- [63] Ç. Yalçınkaya, H. Yazıcı, Effects of ambient temperature and relative humidity on early-age shrinkage of UHPC with high-volume mineral admixtures, *Constr. Build. Mater.* 144 (2017) 252–259.
- [64] Hao Huang, Guang Ye, Examining the “time-zero” of autogenous shrinkage in high/ultra-high performance cement pastes, *Cem. Concr. Res.* 97 (2017) 107–114.
- [65] A. Bentur, S.I. Igarashi, K. Kovler, Prevention of autogenous shrinkage in high-strength concrete by internal curing using wet lightweight aggregates, *Cem. Concr. Res.* 31 (11) (2001) 1587–1591.
- [66] Y. Wang, Z. Shui, Y. Huang, et al., Properties of coral waste-based mortar incorporating metakaolin: Part II. Chloride migration and binding behaviors, *Constr. Build. Mater.* 174 (2018) 433–442.
- [67] X. Wang, R. Yu, Z. Shui, et al., Development of a novel cleaner construction product: ultra-high performance concrete incorporating lead-zinc tailings, *J. Cleaner Prod.* 196 (2018) 172–182.
- [68] Y. Zhang, W. Zhang, J. Liu, Ultra-High Performance Cementitious Composites, Science press, Beijing, China, 2014 (in Chinese).
- [69] E.I. Tazawa, S. Miyazawa, Experimental study on mechanism of autogenous shrinkage of concrete, *Cem. Concr. Res.* 25 (8) (1995) 1633–1638.
- [70] K. Kurumisawa, K. Tanaka, Three-dimensional visualization of pore structure in hardened cement paste by the gallium intrusion technique, *Cem. Concr. Res.* 36 (2) (2006) 330–336.
- [71] L.A. Sbia, A. Peyvandi, P. Soroushian, et al., Evaluation of modified-graphite nanomaterials in concrete nanocomposite based on packing density principles, *Constr. Build. Mater.* 76 (1) (2015) 413–422.
- [72] S. Lu, E.N. Landis, D.T. Keane, X-ray microtomographic studies of pore structure and permeability in Portland cement concrete, *Mater. Struct.* 39 (6) (2006) 611–620.
- [73] W. Shen, Z. Yang, L. Cao, et al., Characterization of manufactured sand: particle shape, surface texture and behavior in concrete, *Constr. Build. Mater.* 114 (2016) 595–601.
- [74] Karen L. Scrivener, Alison K. Crumbie, Peter Laugesen, The interfacial transition zone (ITZ) between cement paste and aggregate in concrete, *Interface Sci.* 12 (4) (2004) 411–421.
- [75] F. Wang, J. Yang, S. Hu, et al., Influence of superabsorbent polymers on the surrounding cement paste, *Cem. Concr. Res.* 81 (2016) 112–121.
- [76] P. Vargas, O. Restrepo-Baena, J.I. Tobón, Microstructural analysis of interfacial transition zone (ITZ) and its impact on the compressive strength of lightweight concretes, *Constr. Build. Mater.* 137 (2017) 381–389.